J. H. Davidson

W. T. Carlson

W. S. Duff

Solar Energy Applications Laboratory,
Colorado State University,
Fort Collins, Colorado 80523

P. J. Schaefer

W. A. Beckman

S. A. Klein

Solar Energy Laboratory,
University of Wisconsin,
Madison, WI

# Comparison of Experimental and Simulated Thermal Ratings of Drain-Back Solar Water Heaters

*Short-term experimental tests of drain-back solar water heaters are compared to ratings obtained using TRNSYS to determine if computer simulations can effectively replace laboratory thermal ratings of solar domestic hot water heating systems. The effectiveness of TRNSYS in predicting changes in rating due to limited changes in collector area, collector flow rate, recirculation flow rate, storage tank volume, and storage tank design is validated to within ±10 percent. Storage tank design is varied by using a stratification manifold in place of the standard drop tube. Variations in other component sizes and operating factors are based on current industry standards.*

## Introduction

Certification of solar domestic hot water (DHW) systems by the Solar Rating and Certification Corporation (SRCC), has until recently relied on a four-day laboratory test which must be repeated if component or operating modifications are made (SRCC, 1984a,b). An alternate, and more cost-effective rating methodology now relies heavily on computer simulations (SRCC, 1991). To determine the validity of the simulation certification path, experimental ratings of generic drain-back systems (Davidson et al., 1992) are compared with simulated ratings obtained with TRNSYS 13.1 (Klein et al., 1990).

Differences between laboratory and simulated thermal ratings are examined in a two-level, five-factor, half-factorial experimental design in which changes in collector area, collector flow rate, recirculation flow rate (storage-side flow rate between the storage tank and the heat exchanger in the drain-back tank), storage tank volume, and storage tank design are considered in 16 rating trials. Storage tank design is varied by using a rigid porous stratification manifold (Carlson, 1990) in place of a standard drop tube. The two levels of each design/operating factor are shown in Table 1.

## Methodology

The rating procedure follows the SRCC OG-200 standard (1984a,b) with a slight adjustment to the total water heating load to agree with the Federal Trade Commission (FTC) rating procedures for conventional gas and electric hot-water systems (FTC, 1989). Hourly radiation and incidence angle profiles are specified with total daily insolation equal to 17.03 MJ/m$^2$. Cold-water supply, tank ambient, and collector ambient temperatures are maintained at 22°C and water set temperature is held at 55°C. Total daily hot water delivered is 49.8 MJ in equal load-draws of 16.6 MJ at 8:00 a.m., 12:00 noon, and 5:00 p.m.

Daily energy quantities included in a rating and sketched in Fig. 1 include: useful collected energy, $Q_u$; daily hot-water energy delivered by the solar storage tank, $Q_s$; parasitic energy, $Q_{par}$; energy delivered to the load, $Q_{del}$; and auxiliary energy, $Q_{aux}$. Energy losses are shown for completeness. Not shown in the figure are net energy delivered from the solar storage tank, $Q_{net}$, equal to $Q_s$ minus $Q_{par}$; energy capacity of the system, $Q_{cap}$; and reserve energy capacity, $Q_{res}$. A rating trial is completed when the daily auxiliary energy input, $Q_{aux}$, converges to within three percent, or four days have elapsed. In the case of nonconvergence, a rating is specified by the average daily energies of the last two days. The simulation does not model the reserve capacity, $Q_{res}$, the energy remaining in the solar storage tank at the end of a test, nor energy capacity, $Q_{cap}$, the energy that the system can deliver without solar input.

**Table 1 Levels for each design and operating factor**

| Factor Description | High Level | Low Level |
|---|---|---|
| Collector Flow Rate (l/s) | 0.114 | 0.057 |
| Recirculation Flow Rate (l/s) | 0.095 | 0.047 |
| Collector Area (m$^2$) | 5.56 | 2.78 |
| Storage Tank Volume (l) | 310 | 250 |
| Storage Tank Design | Basic Drop Tube | Stratification Manifold |

Contributed by the Solar Energy Division of THE AMERICAN SOCIETY OF MECHANICAL ENGINEERS for publication in the ASME JOURNAL OF SOLAR ENERGY ENGINEERING.

Manuscript received by the ASME Solar Energy Division, Aug. 1992; final revision, Dec. 1992. Associate Technical Editor: J. Morehouse.

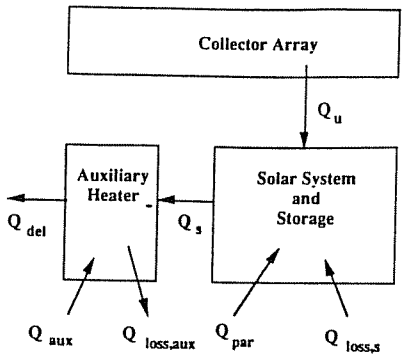


Fig. 1 Schematic of SRCC energy quantities

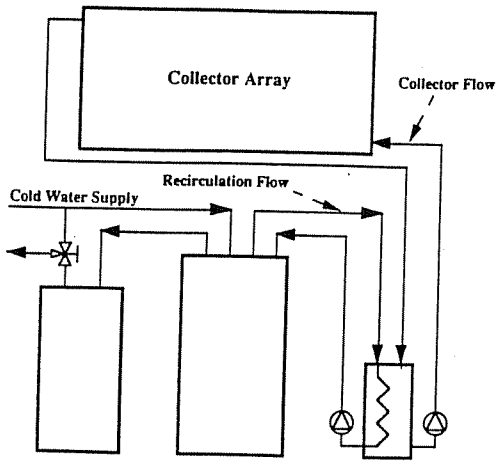


Fig. 2 Schematic of a drain-back solar water heater

A schematic diagram of a generic drain-back system is shown in Fig. 2. (A detailed description of the system is included in Davidson et al., 1992.) Water is the working fluid throughout the system. Although solar collectors are installed in the experimental facility, an electric boiler is used to transfer energy into the system. The Hottel-Whillier equation (with $F_r\,\tau\alpha$ = 0.602, $F_rU_L$ = 5.56 W/m²°C) is used to govern energy delivered by the boiler/collectors in both the experimental and simulation trials. Incidence angle modifier is calculated based on $b_o$ = 0.42. Likewise, both the experiments and simulations emulate a dead-band controller with turn-on and turn-off temperature differences of 11 and 3°C, respectively.

Standard models found in the TRNSYS library are used to model the system, with two exceptions. The pump model is modified, so that for both pumps, 85 percent of the pump work acts to raise the fluid temperature. Power inputs to the pumps are determined from the experiments and for both the collector-side and tank-side loops are nearly constant, regardless of the flow rate. Parasitic energy is calculated as the measured pump power times the simulated pump on-time. The second nonstandard TRNSYS subroutine is the load-flow on-off controller. The controller subroutine turns the flow on at the time step closest to the specified draw time and turns the flow off at the time step in which the simulated energy draw is closest to 16,603 kJ.

Simulated ratings are obtained using measured values of solar storage tank volume and loss coefficient, auxiliary DHW loss coefficient, pipe diameter and length, pump power, and heat exchanger effectiveness, but the degree of tank stratification, drain-back and auxiliary tank volumes, and loss coefficients of the piping and drain-back tank are assumed. Loss coefficient of the drain-back tank is set equal to 0.67 W/°C. Based on measured versus rated volumes of the solar storage tanks, volumes of the auxiliary tank and drain-back tank are assumed to be ten percent less than the rated values listed in Table 1. The submerged coil heat exchanger is modeled as a constant effectiveness exchanger located outside the drain-back tank with an effectiveness equal to the average measured value over the last day of each experimental trial. Only pipe losses between the collector and drain-back tank are included in the simulations. Total length of neglected piping is 4.5 m. Nominal overall resistance of the pipe insulation is increased by approximately six percent to account for actual convection losses.

A major simulation question concerns what type of tank model to use. Kleinbach (1990; Kleinbach, et al., 1991) investigated experimental data for the eight (out of 16) trials without a stratification manifold and concluded that a multimode model, which models the tank as $N$ fully mixed volume segments, predicts tank temperatures and energy delivery better

## Nomenclature

$A$ = area, m²
$b_o$ = constant used in incidence angle modifier calculation
$f$ = design or operating factor (see Fig. 7)
$F_r$ = collector heat removal factor
$K_{\tau\alpha}$ = empirical incident angle modifier
$M$ = mass flow rate, kg/s
$N$ = number of nodes in simulation tank model
Pump percent = percentage of pump work used to raise fluid temperature
$Q$ = daily energy, kJ
$SF$ = solar fraction
$U$ = conductance, W/m²°C
$UA$ = overall heat transfer coefficient, W/°C
$U_L$ = collector heat loss coefficient, W/m²°C
$V$ = volume, l

**Greek Letters**

$\epsilon$ = heat exchanger effectiveness
$\sigma$ = standard error
$\tau\alpha$ = transmittance absorptance product for collector

**Subscripts**

aux = auxiliary
$c$ = collector
cap = refers to energy capacity of system without solar input
$d$-$b$ = drain-back tank
del = refers to hot water energy delivered by system
loss = energy loss
$n$ = normal
net = net energy delivered from preheat tank
par = parasitic energy consumption
$rc$ = refers to recirculation flow rate
res = reserve energy in preheat tank at end of test sequence
$s$ = solar, refers to hot water energy delivered from preheat tank
tank = refers to solar storage tank
$u$ = useful, refers to useful energy gain of fluid through collector array

Table 2 Summary of numerical results

| Trial | Collector Flow Rate (l/s) | Recircula-tion Flow Rate (l/s) | Collector Area ($m^2$) | Storage Tank Volume (l) | Storage Tank Design | SF (%) | $Q_{del}$ (kJ) | $Q_s$ (kJ) | $Q_{net}$ (kJ) | $Q_{aux}$ (kJ) | $Q_{par}$ (kJ) | $Q_u$ (kJ) |
|---|---|---|---|---|---|---|---|---|---|---|---|---|
| 1 | .057 | .047 | 2.78 | 250 | Basic | 20.8 | 49780 | 15900 | 10365 | 39140 | 5535 | 18130 |
| 2 | .114 | .047 | 2.78 | 250 | Manifold | 23.9 | 49780 | 17350 | 11910 | 37690 | 5440 | 18980 |
| 3 | .057 | .095 | 2.78 | 250 | Manifold | 22.2 | 49780 | 16470 | 11070 | 38570 | 5440 | 18490 |
| 4 | .114 | .095 | 2.78 | 250 | Basic | 23.0 | 49780 | 16850 | 11450 | 38180 | 5400 | 18870 |
| 5 | .057 | .047 | 5.56 | 250 | Manifold | 40.1 | 49780 | 25370 | 19970 | 29670 | 5400 | 30620 |
| 6 | .114 | .047 | 5.56 | 250 | Basic | 40.1 | 49780 | 25380 | 19980 | 29660 | 5400 | 30970 |
| 7 | .057 | .095 | 5.56 | 250 | Basic | 38.6 | 49780 | 24600 | 19200 | 30440 | 5400 | 30370 |
| 8 | .114 | .095 | 5.56 | 250 | Manifold | 43.1 | 49780 | 26830 | 21430 | 28210 | 5400 | 32110 |
| 9 | .057 | .047 | 2.78 | 310 | Manifold | 21.9 | 49780 | 16690 | 10919 | 38350 | 5771 | 18680 |
| 10 | .114 | .047 | 2.78 | 310 | Basic | 21.9 | 49780 | 16410 | 10872 | 38630 | 5538 | 18650 |
| 11 | .057 | .095 | 2.78 | 310 | Basic | 20.7 | 49780 | 15840 | 10308 | 39200 | 5532 | 18290 |
| 12 | .114 | .095 | 2.78 | 310 | Manifold | 23.8 | 49780 | 17250 | 11850 | 37790 | 5400 | 19200 |
| 13 | .057 | .047 | 5.56 | 310 | Basic | 37.7 | 49780 | 24150 | 18750 | 30890 | 5400 | 30140 |
| 14 | .114 | .047 | 5.56 | 310 | Manifold | 43.2 | 49780 | 26890 | 21490 | 28150 | 5400 | 32280 |
| 15 | .057 | .095 | 5.56 | 310 | Manifold | 40.1 | 49780 | 25360 | 19960 | 29680 | 5400 | 31160 |
| 16 | .114 | .095 | 5.56 | 310 | Basic | 40.8 | 49780 | 25690 | 20290 | 29350 | 5400 | 31650 |

Table 3 Differences in measured and simulated results as a percentage of measured values (measured-simulated) measures × 100

| Trial | Collector Flow Rate (l/s) | Recircula-tion Flow Rate (l/s) | Collector Area ($m^2$) | Storage Tank Volume (l) | Storage Tank Design | ΔSF (%) | $\Delta Q_{del}$ (%) | $\Delta Q_s$ (%) | $\Delta Q_{net}$ (%) | $\Delta Q_{aux}$ (%) | $\Delta Q_{par}$ (%) | $\Delta Q_u$ (%) |
|---|---|---|---|---|---|---|---|---|---|---|---|---|
| 1 | .057 | .047 | 2.78 | 250 | Basic | 7.6 | -0.1 | 4.5 | 8.0 | 0.5 | 1.8 | -3.3 |
| 2 | .114 | .047 | 2.78 | 250 | Manifold | 8.1 | -0.1 | 11.2 | 8.9 | -6.2 | 17.1 | -4.3 |
| 3 | .057 | .095 | 2.78 | 250 | Manifold | 7.5 | -0.1 | 8.4 | 8.0 | -3.9 | 10.4 | -1.3 |
| 4 | .114 | .095 | 2.78 | 250 | Basic | 0 | -0.1 | 0.9 | 0.1 | 0.0 | 2.4 | -2.5 |
| 5 | .057 | .047 | 5.56 | 250 | Manifold | 1.7 | -0.1 | 3.8 | 1.8 | -1.2 | 10.8 | -4.3 |
| 6 | .114 | .047 | 5.56 | 250 | Basic | -1.2 | -0.1 | 0.4 | 1.4 | -0.4 | 1.1 | -0.9 |
| 7 | .057 | .095 | 5.56 | 250 | Basic | -4.3 | -0.1 | -1.4 | -1.6 | 3.2 | -0.0 | -1.9 |
| 8 | .114 | .095 | 5.56 | 250 | Manifold | -1.9 | -0.1 | 1.6 | -2.0 | 0.6 | 12.9 | -6.9 |
| 9 | .057 | .047 | 2.78 | 310 | Manifold | 12.0 | -0.1 | 9.6 | 13.5 | -2.9 | 4.9 | -2.5 |
| 10 | .114 | .047 | 2.78 | 310 | Basic | 9.1 | -0.1 | 7.4 | 10.3 | -2.3 | 3.3 | -3.2 |
| 11 | .057 | .095 | 2.78 | 310 | Basic | 0 | -0.1 | 6.6 | 9.7 | -1.4 | 2.2 | -1.1 |
| 12 | .114 | .095 | 2.78 | 310 | Manifold | 3.3 | -0.1 | 6.7 | 3.4 | -3.0 | 13.3 | -0.1 |
| 13 | .057 | .047 | 5.56 | 310 | Basic | 4.8 | -0.1 | 3.8 | 5.0 | -0.8 | 0.0 | -1.2 |
| 14 | .114 | .047 | 5.56 | 310 | Manifold | -0.0 | -0.1 | 2.9 | -0.0 | -1.8 | 13.1 | -3.1 |
| 15 | .057 | .095 | 5.56 | 310 | Manifold | 4.3 | -0.1 | 5.9 | 4.6 | -3.5 | 11.2 | -3.4 |
| 16 | .114 | .095 | 5.56 | 310 | Basic | 4.2 | -0.1 | 3.8 | 4.6 | -1.2 | 19.8 | 0.3 |

than either plug flow or plume entrainment models. Three nodes are used to simulate the system without a stratification manifold. The eight simulations for the system with a stratification manifold are modeled with a ten-node tank model. Increasing the number of nodes beyond ten results in negligible differences in daily energy quantities.

## Results

**Direct Comparison.** Table 2 lists the system configurations used for all 16 trials and simulation results. Measured minus simulation energy quantities as a percentage of the measured values are shown in Table 3. (Detailed experimental results, including experimental error, are included in Carlson (1990) and Davidson et al. (1992).) Of particular interest are the differences in energy quantities $Q_u$, $Q_s$, $Q_{net}$, and $Q_{aux}$. Both the experimental and simulated trials deliver the correct total energy to the load. Parasitic energy, $Q_{par}$, is merely an indication of pump-on time since the power required by both pumps during operation is nearly constant. Solar fraction, SF, equals $(Q_s - Q_{par})/Q_{del}$.

Scatter plots comparing experimental and simulation values of $Q_u$, $Q_s$, $Q_{net}$, $Q_{aux}$ are shown in Figs. 3 through 6, respectively. Error bands on the experimental data are two standard deviations of the calculated measurement error. Error bands on $Q_s$, $Q_{net}$, and $Q_{aux}$ include the measurement error for the particular quantity plus the measurement error associated with $Q_u$. This addition of the measurement errors is necessary since any error in energy input directly affects the other energy terms, except for resultant changes in heat loss. Although these scatter plots provide a visual interpretation of the differences between simulated and laboratory ratings of drain-back systems, accuracy of a simulation should not be based on simply whether

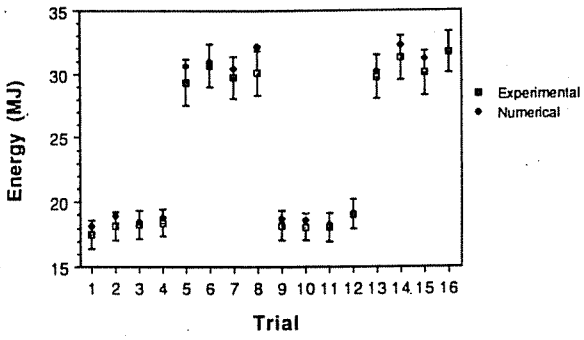


Fig. 3 Comparison of experimental and simulated values of $Q_u$

or not the simulation data fall within measurement error bands since, theoretically, measurements can be made to any degree of accuracy. It is important to consider both the percentage differences as well as the absolute differences.

Both Table 3 and Fig. 3 show good agreement between experimental and numerical values of useful energy collected, $Q_u$. The agreement is expected since $Q_u$ is calculated in both experiment and numerical simulation using the same collector performance model. The only potential discrepancy between the experimental and numerical data is due to differences in collector inlet temperature. Simulated values of $Q_u$ fall within the approximately ±6 percent error bands except in trial #8. As shown in Table 2, the maximum difference in $Q_u$ is less than seven percent of the measured value.

Figure 4 shows that the numerical results are within the experimental error bands of $Q_s$ for the eight trials with high collector area. However, there appears to be a bias between

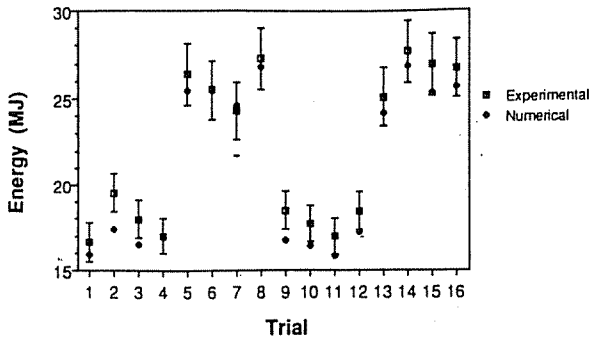


Fig. 4 Comparison of experimental and simulated values of $Q_s$

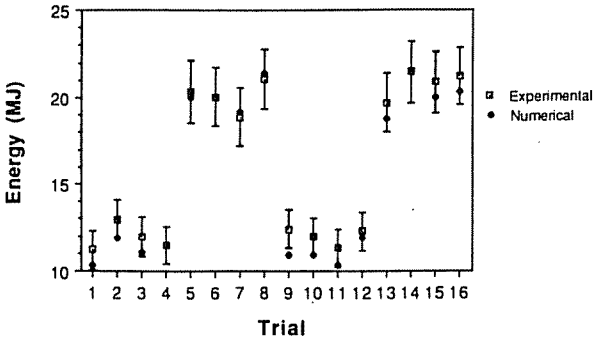


Fig. 5 Comparison of experimental and simulated values of $Q_{net}$

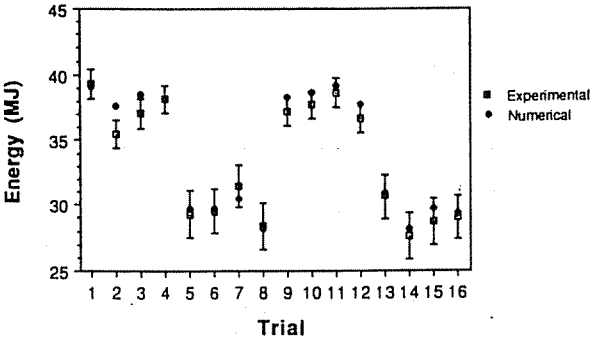


Fig. 6 Comparison of experimental and simulated values of $Q_{aux}$

the experimental and the numerical data in systems with lower ratios of collector area to storage tank volume. The numerical preductions of $Q_S$ are below experimental values in 14 of the 16 simulations, including the eight trials with the smaller collector area (2.78 $m^2$) and the trials with the larger collector area (5.56 $m^2$) in which the larger storage tank (310 liter) is used. The average percent difference between laboratory and simulated values of $Q_S$ is under five percent and the greatest difference is 11 percent.

Comparison of determinations of $Q_{net}$, shown in Fig. 5, indicates that even though the simulation sometimes under predicts $Q_s$, all the simulated calculations of $Q_{net}$ are within the error bands of the experimental values except in trial #9 where the simulated value is low. One trial outside of the error bands is acceptable for a population of 16 when using a $2\sigma$ error. As is the case with $Q_S$, simulated values of $Q_{net}$ are consistently low in the trials in which the ratio of collector area to storage tank volume is low. In assessing the effectiveness of the simulation, $Q_s$ is a better tool than $Q_{net}$ since differences in $Q_{net}$ are due to differences in both $Q_s$ and pump on-time. This is particularly true when using hourly insolation profiles. Pump-on times are either exactly the same or differ by one hour.

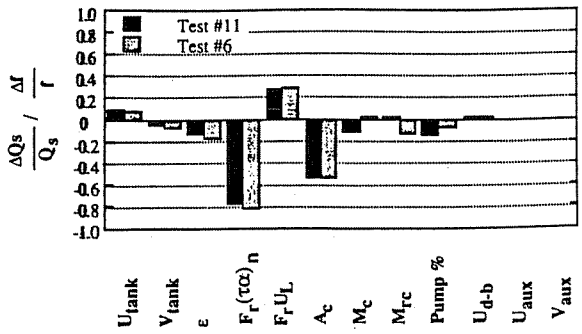


Fig. 7 Sensitivity analysis for trials #6 and #11

Although solar energy output is sometimes under predicted by the simulation, the data plotted in Fig. 6 indicate that except for trial #2, simulated values of $Q_{aux}$ lie within the error bands and are within four percent of the experimental values. The fact that the experimental and simulation values of $Q_{aux}$ are close despite larger differences in $Q_s$ is an indication that losses from the auxiliary heater differ.

The biases between experimental and simulated values of $Q_s$ limit the simulation's ability to predict energy output to a higher degree of accuracy than $\pm 10$ percent. The bias may be due to several factors other than instrumentation. Even well-controlled experiments do not achieve steady-periodic conditions in a four-day test period. Hence, a bias exists when test results are compared to simulations that are necessarily steady-periodic. In addition, it is unknown how much of the pump energy ends up in the fluid and how much is lost to ambient. The differences or biases between experimental and numerical data for the responses $Q_s$ and $Q_{net}$ are well within the magnitude of the pumping energy. Another source of bias could be modeling errors of the heat-loss coefficients for the drain-back module and the piping.

**Simulation Sensitivity Analysis.** A sensitivity analysis to determine the importance of accurately knowing the values of the system parameters used in the simulations is performed with the 12 system parameters listed here being reduced one at a time by ten percent of their nominal value.

1 solar tank's heat-loss coefficient per unit area ($U_{tank}$)
2 solar tank's volume ($V_{tank}$)
3 heat exchanger effectiveness ($\epsilon$)
4 collector gain coefficient at normal irradiance ($F_r(\tau\alpha)_n$)
5 collector loss coefficient per unit area ($F_rU_L$)
6 collector area ($A_c$)
7 collector loop mass flow rate ($M_c$)
8 recirculation loop mass flow rate ($M_{rc}$)
9 percentage of pump work which acts to raise the fluid's temperature (Pump percent)
10 drain-back tank heat-loss coefficient per unit area ($U_{d-b}$)
11 auxiliary tank heat-loss coefficient per unit area ($U_{aux}$)
12 auxiliary tank volume ($V_{aux}$)

Sensitivity analysis results are reported in Fig. 7 in terms of the fractional change of $Q_s$ with respect to a fractional change of a design or operating variable for the conditions of trials #6 and #11. The results emphasize the importance of accurately knowing collector area and the collector parameters $F_r(\tau\alpha)_n$ and $F_rU_L$. Uncertainty in the other variables investigated appears to be of minor importance, even for heat exchanger effectiveness. For reasonably effective heat exchangers, variations in measured heat exchanger effectiveness have only a small effect on simulation results.

## Conclusions

Most appliances sold today, including gas and electric water heaters, include a sticker providing the customer with infor-

mation concerning the typical annual cost of operating the appliance. Similar information should be provided to potential customers of solar water-heating systems. However, the variability in climate makes the preparation and interpretation of such sticker information more difficult. The cost of experimentally determining solar water-heating system performance in each climate necessitates the use of computer simulations to obtain site-specific performance data. The results of this paper demonstrate that carefully formulated computer simulations can provide results which agree well with experimental data. Once validated, a simulation can be used to provide performance rating information needed by potential solar water-heating system customers.

## Acknowledgments

The support of this work by the United States Department of Energy Solar Heating and Cooling Research and Development Office is gratefully acknowledged.

## References

American Society of Heating, Refrigerating and Air-Conditioning Engineers, Inc., 1987, *Methods of Testing to Determine the Thermal Performance of Solar Domestic Water Heating Systems*, Standard 95-1987. Atlanta, GA.

Carlson, W. T., 1990, "Comparison of Experimental and TRNSYS SRCC Ratings of a Generic Drain Back Solar Water System," Masters Thesis, Colorado State University.

Davidson, J. H., Duff, W. S., and Carlson, W. T., 1992, "Impact of Component Selection and Operation on Thermal Ratings of Drain-Back Solar Water Heaters," ASME JOURNAL OF SOLAR ENERGY ENGINEERING, Vol. 114, pp. 219–226.

Federal Trade Commission, 1989, "Uniform Test Method for Measuring the Energy Consumption of Water Heaters," Code of Federal Regulations, 10 CFR Ch II, Part 430, Subpart B, Appendix E.

Klein, S. A., et al., 1990, "TRNSYS, A Transient Simulation Program, 13.1 User's Manual," Report 38-13, Solar Energy Laboratory, University of Wisconsin, Madison.

Kleinbach, E. M., 1990, "Performance Study of One-Dimensional Models for Stratified Thermal Storage Tank," Masters Thesis, University of Wisconsin, Madison, Wisconsin.

Kleinbach, E. M., Beckman, W. A., and Klein, S. A., 1991, "Performance of One-Dimensional Models for Stratified Thermal Storage Tanks," *Solar World Congress, Proceedings of the Biennial Congress of the International Solar Energy Conference*, Vol. 2, Part I, pp. 1397–1402.

Solar Rating and Certification Corporation, Washington, D.C., 1984a, "Operating Guidelines for Certifying Solar Water Heating Systems," Document OG-200, (Nov.).

Solar Rating and Certification Corporation, Washington, D.C., 1984b, "Test Methods and Minimum Standards for Certifying Solar Water Heating Systems," Standard 200-82.

Solar Rating and Certification Corporation, Washington, D.C., 1991, "Operating Guidelines and Minimum Standards for Certifying Solar Water Heating Systems: An Optional SWH System Certification and Rating Program, Document OG-300-91, (Nov.).